PAPER

NJC
www.rsc.org/njc

Microwave effects on the electrochemical deposition of copper

Ujjal Kumar Sur,[a] Frank Marken,*[a] Richard G. Compton[b] and Barry A. Coles[b]

[a] *Department of Chemistry, Loughborough University, Loughborough, UK LE11 3TU. E-mail: F.Marken@Lboro.ac.uk; Fax: 01509 22 3925; Tel: 01509 22 2551*
[b] *Physical & Theoretical Chemistry Laboratory, Oxford University, Oxford, UK OX1 3QZ*

Received (in Durham, UK) 28th July 2004, Accepted 20th October 2004
First published as an Advance Article on the web 16th November 2004

The effects of microwave radiation on the electro-deposition of copper metal on platinum, gold, and carbon electrode surfaces are studied by cyclic voltammetry and scanning electron microscopy. Electrochemical experiments under microwave conditions are carried out in a conventional three-electrode electrochemical cell placed into a 2.45 GHz microwave cavity. The microwave effect is associated with steady state electrode temperatures of up to 400 K and mass transport enhancements, which are both electrode size and electrode material dependent. The most dramatic mass transport effects are observed at 25 μm diameter platinum microelectrodes with limiting current increases of more than two orders of magnitude. The morphology of the copper deposit at 50 μm diameter platinum electrodes is shown to change from dendritic to cauliflower-type at high microwave intensities. *In situ* thermal de-complexation of Cu^{2+} cations in the presence of a strong complexing agent bovine serum albumin (BSA) is achieved under the microwave conditions.

1. Introduction

Microwave heating provides an emerging and versatile activation tool in chemistry[1] and can lead to localized superheating and inverted temperature gradients.[2] Microwave activation has been employed to promote catalysis,[3] organic and inorganic syntheses,[4] plasma reactions, analytical sample processing, and ceramic sintering. In addition to affecting homogeneous chemical processes, microwave activation has been reported to modify processes at interfaces[5] and in heterogeneous systems.[6]

The *in situ* microwave activation of electrochemical processes has been observed in an electrochemical flow cell system,[7] in which intense microwave radiation is self-focused into a small region within the diffusion layer at the working electrode | solution (electrolyte) interface.[8] Applications of microwave activation have been proposed for example in electroanalysis.[9] An oversimplified physical model for the microwave focusing and activation effects based on Joule heating has been proposed to quantitatively account for the observed electrochemical currents.[10] It has been shown that in the high temperature zone at the electrode surface, mass transport is enhanced in about equal amounts by (i) the temperature effect on rate of diffusion and (ii) by additional convection in the presence of temperature and viscosity gradients.

Recently, microwave activation has been employed for the deposition of Pb metal and PbO_2 on glassy carbon and boron-doped diamond electrodes.[11] For both types of electrodes, the effects have been inferred as predominantly thermal in nature and dramatic improvement for the deposition and stripping of PbO_2 on BDD has been observed in the presence of microwaves. In the present study, the effect of microwave radiation on the copper deposition and stripping processes at carbon, platinum, and gold microelectrodes is investigated and compared. Effects due to the electrode diameter and material are discussed and the effects of microwave heating on the de-complexation of Cu^{2+} in the presence of bovine serum albumin are explored as a model system for beneficial effects of microwave activation in electroanalysis. A dramatic morphology change of the copper deposit going from modest to extreme microwave activation conditions is observed. Under high microwave intensity conditions a change from dendritic to cauliflower-type growth occurs consistent with a very high rate of nucleation.

2. Experimental

2.1. Reagents

Copper sulfate, $K_4Fe(CN)_6$, (Fisons), $K_3Fe(CN)_6$ (BDH), K_2SO_4 (Aldrich), sulfuric acid (Fisher), bovine serum albumin (Sigma) were obtained in the purest commercially available grade and used without further purification. Millipore water with a resistivity of not less than 18 MΩ cm was taken from a Milli-Q water purification system.

2.2. Instrumentation

Images from field emission gun scanning electron microscopy (FEGSEM) were obtained on a Leo 1530 field emission gun SEM system. For electrochemical experiments, a μ-Autolab II potentiostat (Eco Chemie, Netherlands) was employed. The electrochemical system is based on a three-electrode electrochemical flow cell, which is placed through a port into the microwave cavity (see Fig. 1A). The working electrode of the conventional electrochemical cell is located in the microwave cavity and electrochemical experiments are performed as a function of microwave intensity (controlled by setting the magnetron anode current). The electrochemical cell consists of a three-electrode arrangement with a large area Pt gauze as downstream counter electrode, a saturated calomel electrode (SCE) as upstream reference electrode and a microwave working electrode (platinum, gold or carbon fiber microelectrodes of diameter 50 μm, 25 μm or 33 μm were employed). The microelectrodes were fabricated by sealing a coiled Pt wire[12] together with gold microwire or glassy carbon microfiber (33 μm diameter, monofilament glassy carbon, Avco Cooperation, US) into glass (Micro Glass Instruments, Greensborough, Victoria, Australia). A test with a radiation meter (Apollo XI microwave monitor, Apollo Ltd) confirmed the design to act as a filter minimising microwave radiation conduction out of the

DOI: 10.1039/b411536h

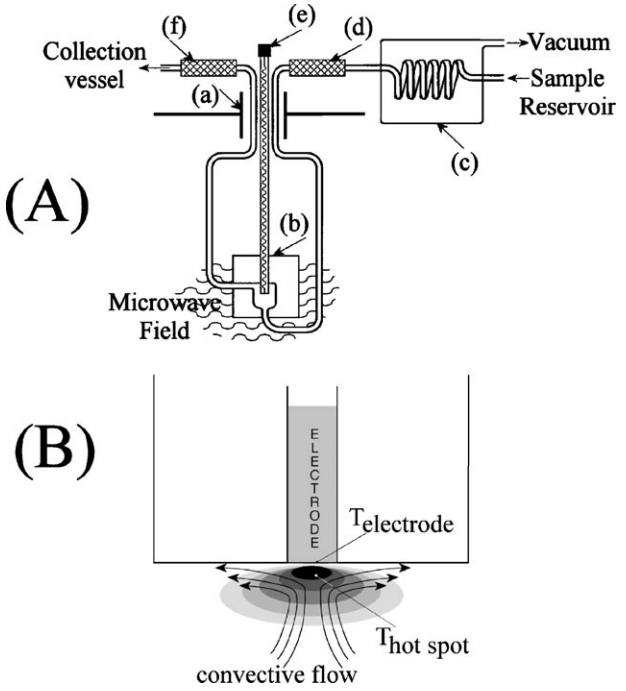

Fig. 1 (A) Electrochemical system for microwave enhanced voltammetry: (a) port for electrochemical cell, (b) flow cell connected to Viton™ inlet/outlet tubing, (c) vacuum degassing system with Goretex™ tubing, (d) reference electrode, (e) working electrode, and (f) Pt gauze counter electrode. (B) Schematic representation of the thermal and convective effects induced by focused microwaves.

cavity. For microwave activation experiments, a multi-mode microwave oven (Panasonic NN-3456, 2.45 GHz) with modified smooth power supply, a water energy sink, and a port for the electrochemical cell was used. *Note that bringing metal objects into a microwave cavity is dangerous. Before operation, the system was tested for leaking microwave radiation with a radiation meter.*

A vacuum degassing step proved to be crucial for high temperature voltammetric experiments (see Fig. 1A). Electrolyte solution coming from the reservoir was passed through 40 cm length 3 mm diameter GoreTex™ tubing (W. L. Gore & Associates UK Ltd, Livingston) placed in an oil-pump evacuated cell. In this way, the gas vapour pressure was dramatically reduced and gas-bubble formation during heating suppressed. During experiments, a slow flow of electrolyte solution (*ca.* 0.65 ml min^{-1}) through the electrochemical cell was maintained to minimize bulk solution heating within the cell and to avoid overheating of the inlet and outlet solution.

3. Results and discussion

3.1. Temperature calibration in the presence of microwave radiation

First, a calibration of the electrode surface temperature $T_{electrode}$ was performed based on the ferrocyanide/ferricyanide redox system (0.1 M K_2SO_4 at pH 3). A thermostatted solution (the reference electrode and the counter electrode were kept outside without thermostatting) of 2 mM $K_3Fe(CN)_6$ and 2 mM $K_4Fe(CN)_6$ in 0.1 M K_2SO_4 at pH 3 exhibits an equilibrium potential which is approximately linearly related to the solution temperature and independent of the electrode size or material used. Data over a temperature range from 298 K to 363 K were obtained and a temperature coefficient $dE^{0\prime}/dT = -1.19$ mV K^{-1} was obtained.

In the presence of microwaves, strong thermal effects are observed which have been attributed to microwave self-focusing at the tip of the electrode immersed in the solution phase.[13]

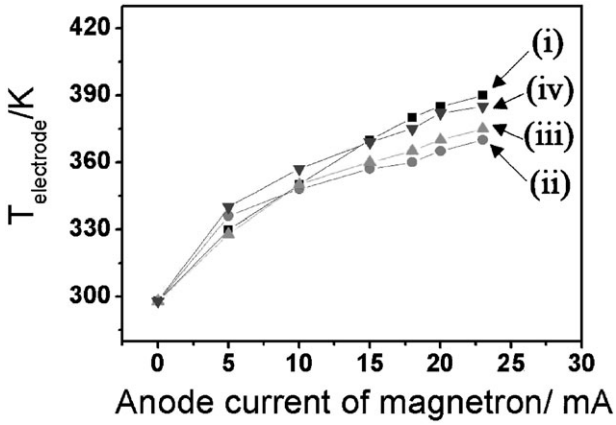

Fig. 2 Plot of the variation of $T_{electrode}$ (determined from the zero current potential for the $Fe(CN)_6^{3-/4-}$ redox system in 0.1 M K_2SO_4 (pH 3) with $dE^{0\prime}/dT = -1.19$ mV K^{-1}) for different electrodes and at different microwave power settings: (i) 25 μm diameter Pt microdisk electrode, (ii) 50 μm diameter Pt microdisk electrode, (iii) 50 μm diameter Au microdisk electrode, and (iv) 33 μm diameter glassy carbon microfiber electrode.

A high temperature region forms (see Fig. 1B) and the temperature at the electrode surface $T_{electrode}$ strongly deviates from the bulk solution temperature. Under these conditions, the temperature at the electrode, $T_{electrode}$, can again be (approximately, ignoring the Soret effect[14] and junction potentials within the heated electrode) determined based on measurements of the equilibrium potential for the $Fe(CN)_6^{3-/4-}$ redox couple. However, the temperature in the solution phase, $T_{hot\ spot}$, cannot be determined directly. Fig. 2 shows the calibration plot of $T_{electrode}$ values for different types of electrodes and at different microwave power settings (the magnetron anode current was employed to vary the microwave power). Similar 'steady state' temperature effects are observed at all the electrodes and a threshold for the 'steady state' high temperature limit for $T_{electrode}$ appears to be at *ca.* 400 K. The fact that this high temperature limit is attained more easily at smaller electrodes can be explained by the smaller solution volume affected and better microwave focusing.

3.2. Microwave effects on the copper deposition and stripping processes at Pt, Au and carbon electrodes

Copper in an acidic sulfate-based electrolyte solution exists as aqua complex and is reduced at an electrode at a sufficiently negative potential in two consecutive one electron transfer processes to copper metal (see eqns. 1 and 2). The deposition process can be reversed by application of potentials positive of the deposition potential.

$$Cu^{2+}\ (aq) + e^- \rightarrow Cu^+\ (aq) \quad (1)$$

$$Cu^+\ (aq) + e^- \rightarrow Cu\ (s) \quad (2)$$

Fig. 3A (i) (inset) shows the cyclic voltammogram obtained for the reduction of 2 mM $CuSO_4$ in 0.1 M K_2SO_4 (pH = 3). Copper deposition and dissolution reactions occur in absence of microwave radiation at a 25 μm diameter Pt microelectrode. Copper deposition commences at *ca.* –0.3 V *vs.* SCE and the limiting current for copper deposition process can be estimated as 15 nA. This limiting current is consistent with the expected value based on the equation for the steady state limiting current at a microdisk electrode $I_{lim} = 4nFDrc = 14$ nA with $n = 2$, the number of electrons transferred per molecule diffusing to the electrode, F, the Faraday constant, $D_{Copper} = 0.72 \times 10^{-9}$ m^2 s^{-1}, the diffusion coefficient,[15] $r = 12.5$ μm, the electrode radius, and $c = 2$ mol m^{-3}, the concentration. After reversing the potential scan a stripping response for the copper dissolution is detected commencing at *ca.* 0.0 V *vs.* SCE.

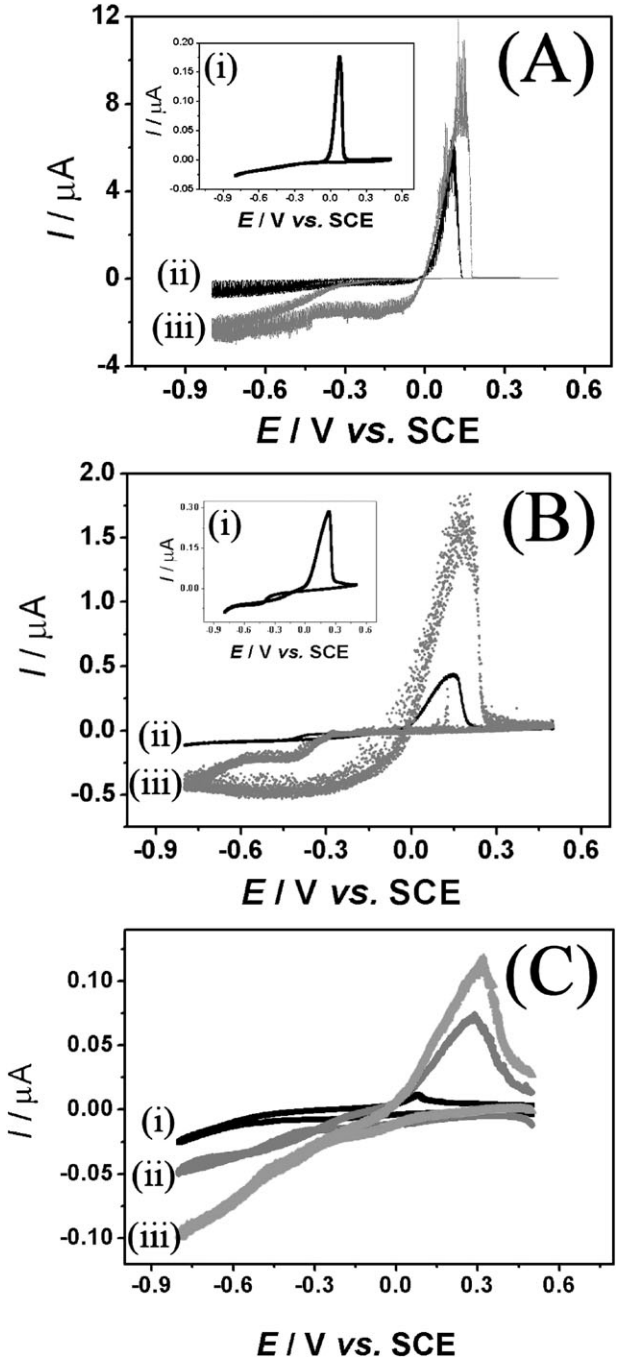

Fig. 3 (A) Cyclic voltammograms (scan rate 0.1 V s^{-1}) for the reduction of 2 mM $CuSO_4$ in 0.1 M K_2SO_4 (pH 3) at a 25 μm diameter Pt microdisk electrode at microwave power settings of (i) 0, (ii) 5 and (iii) 10 mA magnetron anode current. (B) Cyclic voltammograms (scan rate 0.1 V s^{-1}) for the reduction of 2 mM $CuSO_4$ in 0.1 M K_2SO_4 (pH 3) at a 50 μm diameter Au microdisk electrode at microwave power settings of (i) 0, (ii) 5 and (iii) 10 mA magnetron anode current. (C) Cyclic voltammograms (scan rate 0.01 V s^{-1}) for the reduction of 2 mM $CuSO_4$ in 0.1 M K_2SO_4 (pH 3) at a 33 μm diameter glassy carbon microfiber electrode at microwave power settings of (i) 0, (ii) 5 and (iii) 10 mA magnetron anode current.

Fig. 3A (ii) and 3A (iii) show cyclic voltammograms obtained in the presence of microwave radiation at anode currents of 5 and 10 mA, respectively. From the calibration plot in Fig. 2 it can be seen that these conditions correspond to electrode temperatures of $T_{electrode}$ = 330 K and 350 K, respectively. In the presence of microwave radiation, copper deposition commences at essentially the same potential but there is an enhancement of both the copper deposition limiting current and copper dissolution current. The limiting current for the copper deposition process reaches a value of 2.14 μA at a microwave power of 10 mA magnetron anode current (enhancement factor 126) and can be further increased at higher microwave power. This behaviour is consistent with a recent study showing that the mass transport limited current for electrode processes can be enhanced up to three orders of magnitude in the presence of microwave radiation.[7] The physical mechanism responsible for this massively enhanced current is probably the formation of a steam bubble and fast convective mass transport at the resulting gas | liquid interface. It is interesting to note the effect of the microwave radiation on the copper stripping response. At intermediate microwave power substantially higher stripping signals are observed in agreement with the increase of mass transport and amount of copper deposited. However, when going to higher microwave power settings (see Fig. 3A (iii)) only insignificant improvements in the stripping signal are observed. It is believed that under conditions of fast mass transport and high temperatures, reduced forms of copper can escape from the electrode surface into the bulk solution (*vide infra*).

Fig. 3B (i–iii) show cyclic voltammograms obtained for the reduction of 2 mM Cu^{2+} at a 50 μm diameter gold electrode. Similar trends are observed, but the effect of applying 5 mA and 10 mA magnetron anode current (corresponding to $T_{electrode}$ = 330 K and 350 K, respectively) is less dramatic in mass transport. Overall the limiting current for the deposition process increases by only one order of magnitude. Similar results are obtained at a 50 μm diameter platinum electrode and are attributed to a purely thermal increase in diffusion and convection.

In Fig. 3C (i)–(iii) cyclic voltammograms obtained for the reduction of 2 mM Cu^{2+} at a 33 μm diameter glassy carbon electrode in the absence and in the presence of microwave radiation are shown. The temperature at the electrode surface, $T_{electrode}$, in the presence of microwave radiation with 5 mA and 10 mA magnetron current is 340 K and 357 K, respectively, and therefore higher than that observed at the metal electrodes (see Fig. 2). However, it has been shown recently that the microwave interaction with carbon causes direct heating[16] and therefore only modest effects are observed in the solution phase. Both the limiting current for reduction and the stripping peak current are enhanced, but the mass transport effects are relatively small.

Even under extreme conditions at a 25 μm diameter platinum microelectrode and with high microwave power, Faradaic currents can be shown to be directly proportional to the concentration of Cu^{2+} in solution. Fig. 4 shows voltammograms obtained for concentrations of 2 mM, 0.2 mM and 0.02 mM Cu^{2+} and for all concentrations the enhancement of copper deposition and dissolution current is more or less constant, although background currents start to dominate the copper deposition process at low concentration.

3.3. Electron microscopy investigation of the microwave effect on copper deposition

In order to gain more insight into the copper deposition process in particular in the presence of high intensity microwave radiation, copper deposits were formed and studied by field emission gun scanning electron microscopy (FEGSEM). Fig. 5 shows three cyclic voltammograms for the deposition of 10 mM $CuSO_4$ in 0.1 M K_2SO_4 (pH 3) at a 50 μm diameter Pt microelectrode and in the presence of (A) 0 mA, (B) 10 mA and (C) 20 mA magnetron anode current (consistent with steady state electrode surface temperatures of $T_{electrode}$ = 298 K, 350 K and 365 K). In all three cases copper deposition occurs at a potential of –0.3 V *vs.* SCE and this potential has been chosen for the preparation of samples for microscopy.

Fig. 6A–C show FEGSEM images of copper deposits at a 50 μm diameter Pt microelectrode obtained after 30 min deposition time and at different microwave power settings. In the absence of microwaves during the deposition step only

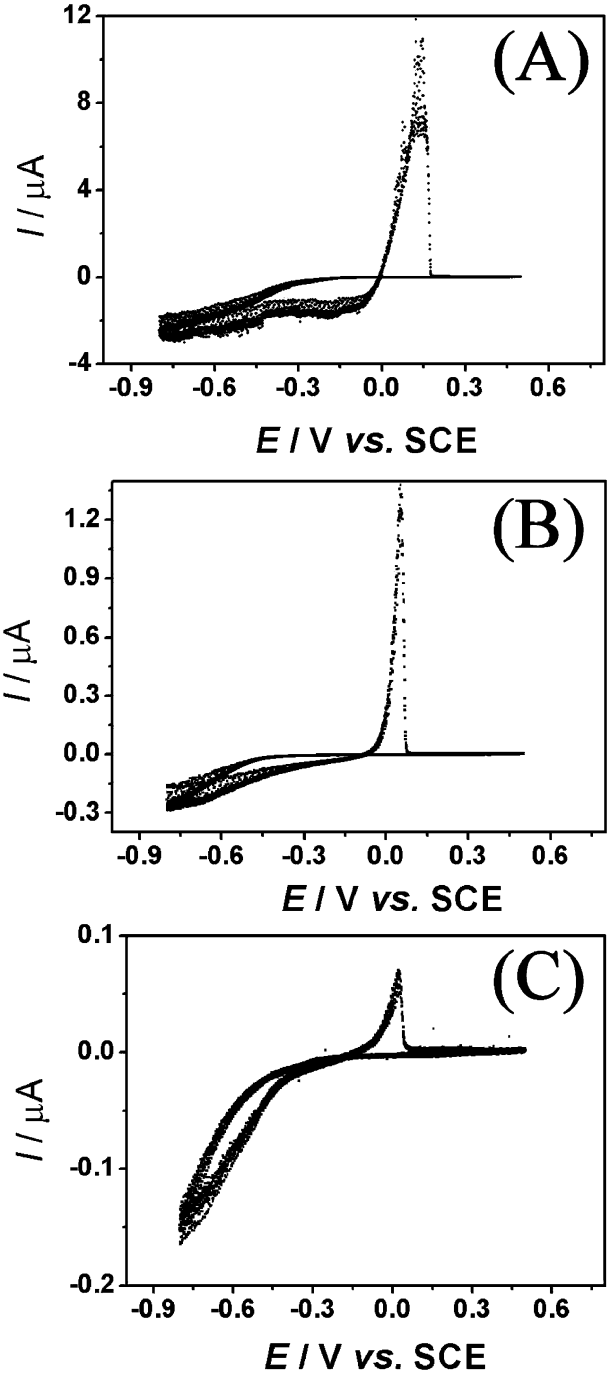

Fig. 4 Cyclic voltammograms (scan rate 0.1 V s^{-1}) for the reduction of $CuSO_4$ in 0.1 M K_2SO_4 (pH 3) at a 25 μm diameter Pt microdisk with (A) 2 mM, (B) 0.2 mM and (C) 0.02 mM $CuSO_4$ in presence of a microwave field (magnetron anode current 10 mA).

some copper metal growth onto the platinum surface is observed. Growth appears to occur predominantly in scratches. In contrast, when deposited in the presence of moderate microwave power (magnetron anode current 10 mA), the platinum surface is fully covered. A dendritic growth pattern is observed with features on the micron scale. Dendritic growth of copper is common and there are various examples in the literature.[17,18] Mass transport is a key factor in causing dendritic growth and controls the relative rates of nucleation *versus* growth. Under moderate microwave power, the morphology of the copper deposit seems controlled by the diffusion process. However, both the applied potential and the temperature also are key factors in controlling nucleation and growth rates.

Next, at high microwave power (magnetron anode current 20 mA) a distinctly different type of copper deposit is observed.

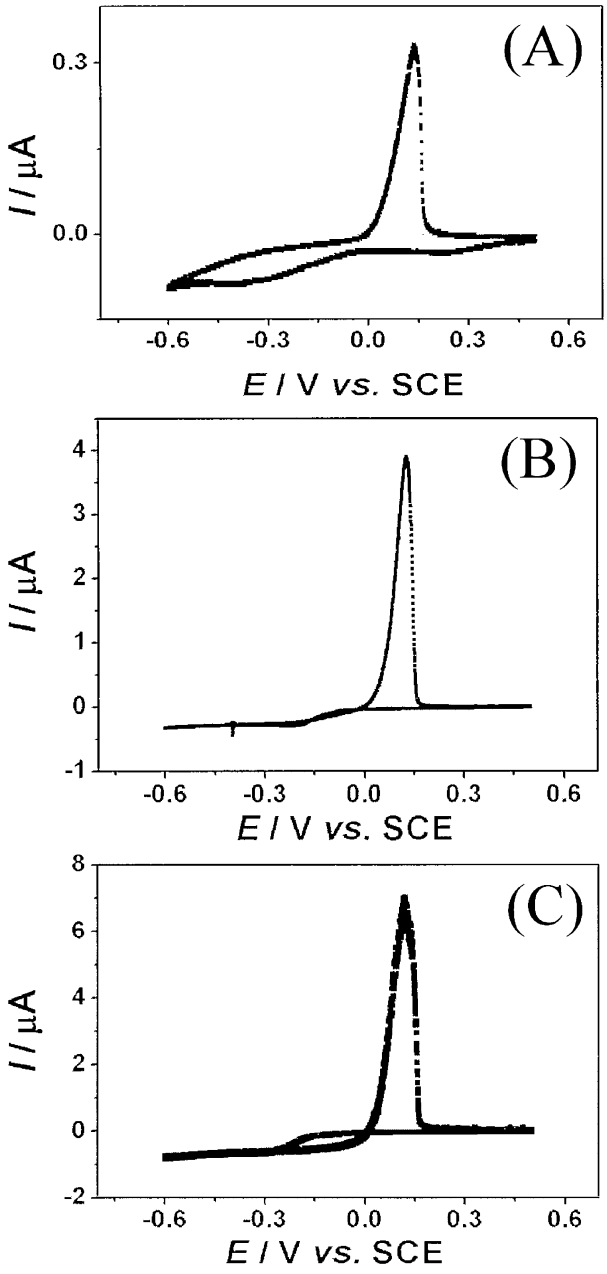

Fig. 5 Cyclic voltammograms (scan rate 0.1 V s^{-1}) for the reduction of 10 mM $CuSO_4$ in 0.1 M K_2SO_4 (pH 3) at a 50 μm diameter Pt microdisk electrode at microwave power settings of (A) 0, (B) 10 and (C) 20 mA magnetron anode current.

Fig. 6C shows the FEGSEM images of a copper deposit formed at a 50 μm diameter Pt microelectrode under otherwise identical conditions. It can be seen from the FEGSEM image that there is cauliflower-like growth of metallic copper on the platinum microelectrode surface. At high microwave power, the rate of nucleation becomes much faster and diffusion control becomes insignificant. Many small nuclei form rapidly and in the image small copper particles of *ca.* 200 nm can be seen as part of the growth. It is possible that this type of growth is responsible for the losses of copper observed during the deposition process in the presence of high microwave intensity (*vide supra*).

3.4. Microwave enhanced deposition of copper in the presence of strongly complexing BSA media

Metal deposition and stripping processes are often employed in analytical contexts[19] in particular for rapid assessing and monitoring of heavy metal or copper impurities.[20] The

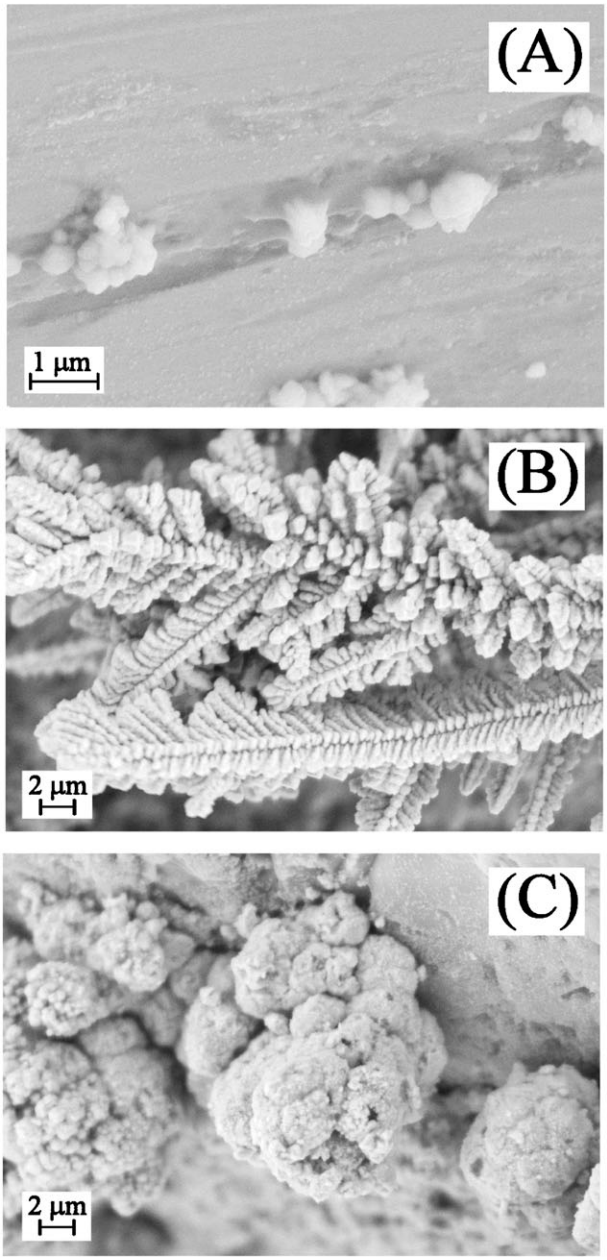

Fig. 6 FEGSEM images of copper deposits formed at a 50 μm diameter Pt microdisk electrode (A) in absence of microwave radiation, (B) in the presence of 10 mA and (C) in the presence of 20 mA magentron anode current. The deposition occurred at a potential of −0.3 V *vs.* SCE in a solution of 10 mM $CuSO_4$ in 0.1 M K_2SO_4 (pH 3) for 30 min.

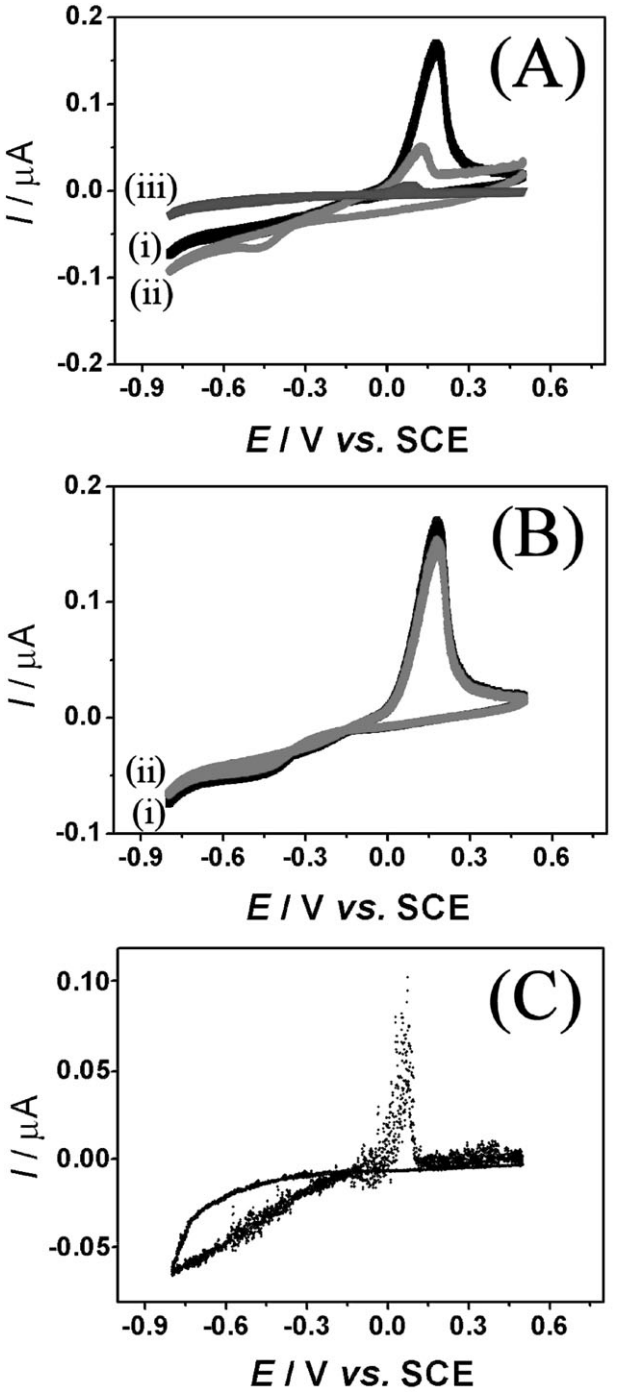

Fig. 7 (A) Cyclic voltammograms (scan rate 0.1 V s^{-1}) for the reduction of 2 mM $CuSO_4$ in 0.1 M K_2SO_4 (pH 3) at a 50 μm diameter Au microdisk electrode in the presence of (i) 0 μM, (ii) 1 μM and (iii) 1000 μM BSA. (B) Cyclic voltammograms for the reduction of 2 mM $CuSO_4$ under the same conditions with (i) a bare gold electrode and (ii) a gold electrode which has been kept in 1 mM BSA solution for 30 min. (C) Cyclic voltammogram obtained at a 50 μm diameter gold microdisk electrode under the same conditions in the presence of 1000 μM BSA and with a microwave power setting of 20 mA magnetron anode current.

nucleation and growth of metals such as copper can be heavily affected by other components of the sample, in particular by proteins. Bovine serum albumin (BSA) is a model system for copper complexation and has been intensely studied.[21] The effect of microwave radiation on the de-complexation of copper is investigated here.

Fig. 7A (i) shows the cyclic voltammograms obtained at a 50 μm diameter Au disk microelectrode for the reduction of 2 mM $CuSO_4$ in 0.1 M K_2SO_4 (pH 3). Complex formation with BSA causes both the deposition current and in particular the stripping response to decrease. Fig. 7A (ii) and 7A (iii) show the voltammograms in presence of 1 μM and 1000 μM BSA with considerably reduced currents. The effect of BSA adsorbed onto the gold electrode surface is insignificant as is shown in Fig. 7B. A layer of BSA adsorbed onto the electrode causes only minor changes in the voltammogram. Therefore complexation of Cu^{2+} in solution seems responsible for effects on the copper deposition. In part, it is possible to apply more negative deposition potentials in order to overcome the complexation effect. However, hydrogen evolution is competing with copper deposition and microwave activation provides an alternative tool to restore the voltammetric response. Fig. 7C shows the voltammogram obtained in the presence of 1000 μM BSA and high microwave power (magnetron anode current 20 mA). The voltammetric response can be restored presumably due to *in situ* de-complexation and fast deposition of

copper metal onto the gold electrode. The electrode process in the presence of the BSA complex may be regarded as CE-type with a microwave enhanced fast chemical de-complexation (C-step) prior to electrochemical reduction of Cu^{2+} (E-step).

4. Conclusions

Microwave radiation offers a new tool in electrochemistry with steady state temperatures in aqueous media of up to 400 K and predominantly thermal effects on processes at small electrodes. Processes at microelectrodes of 25–50 μm diameter can be dramatic with current enhancements of up to three orders of magnitude. It has been shown here that copper deposition processes can be enhanced and that the type of copper growth is affected by the presence of microwave radiation. Although effects observed in this study can be understood as purely thermal, there remain interesting questions concerning the effects of high intensity microwaves for example, at complex surfaces (*e.g.* during metal deposition processes). Further work exploring and quantifying the physico-chemical effects of microwave effects in electrochemistry are in progress. In particular, the high temperature de-complexation effect in the presence of complexing media will be of relevance in electro-analytical applications of microwave activation.

Acknowledgements

F. M. thanks the Royal Society for the award of a University Research Fellowship. W. L. Gore & Associates (UK) Ltd are gratefully acknowledged for the generous supply of porous PTFE tubing. This work was funded by the EPSRC (GR/S06349/01) and undertaken as part of the EU sponsored D32 COST Programme (Microwave and Ultrasound Activation in Chemical Analysis).

References

1 R. Gedye, F. Smith, K. Westaway, H. Ali, L. Balderisa, L. Laberge and J. Rousell, *Tetrahedron Lett.*, 1986, **27**, 279.
2 H. M. Kingston and S. J. Haswell, in *Microwave-Enhanced Chemistry*, American Chemical Society, Washington, 1997.
3 See for example: J. R. Thomas, *Catal. Lett.*, 1997, **49**, 137.
4 See for example: F. Langa, P. De La Cruz, A. De La Hoz, A. Diaz-Ortiz and E. Diez-Barra, *Contemp. Org. Synth.*, 1997, 373.
5 See for example: R. Maoz, H. Cohen and J. Sagiv, *Langmuir*, 1998, **14**, 5988.
6 See for example: P. D. I. Fletcher, D. D. Grice and S. J. Haswell, *Phys. Chem. Chem. Phys.*, 2001, **3**, 1067.
7 U. K. Sur, F. Marken, N. Rees, B. A. Coles, R. G. Compton and R. Seager, *J. Electroanal. Chem.*, 2004, **573**, 175.
8 F. Marken, S. L. Matthews, R. G. Compton and B. A. Coles, *Electroanalysis*, 2000, **12**, 267.
9 Y. C. Tsai, B. A. Coles, K. Holt, J. S. Foord, F. Marken and R. G. Compton, *Electroanalysis*, 2001, **13**, 831.
10 F. Marken, Y. C. Tsai, B. A. Coles, S. L. Matthews and R. G. Compton, *New J. Chem.*, 2000, **24**, 653.
11 F. Marken, Y. C. Tsai, A. J. Saterlay, B. A. Coles, D. Tibbetts, K. Holt, C. H. Goeting, J. S. Foord and R. G. Compton, *J. Solid State Electrochem.*, 2001, **5**, 313.
12 R. G. Compton, B. A. Coles and F. Marken, *Chem. Commun.*, 1998, 2595.
13 Y. C. Tsai, B. A. Coles, R. G. Compton and F. Marken, *J. Am. Chem. Soc.*, 2002, **124**, 9784.
14 J. F. Smalley, C. V. Krishnan, M. Goldman, S. W. Feldberg and I. Ruzic, *J. Electroanal. Chem.*, 1988, **248**, 255.
15 See for example: R. Mills and V. M. M. Lobo, *Self-diffusion in electrolyte solutions*, Elsevier, Amsterdam, 1989.
16 U. K. Sur, F. Marken, R. Seager, J. S. Foord, A. Chatterjee, B. A. Coles and R. G. Compton, *Electroanalysis*, 2004, in print.
17 M. G. Pavlovic, S. Kindlova and I. Rousar, *Electrochim. Acta*, 1992, **37**, 23.
18 K. I. Popov, M. G. Pavlovic and M. D. Maksimovic, *J. Appl. Electrochem.*, 1982, **12**, 525.
19 See for example: J. Wang, *Analytical Electrochemistry*, Wiley-VCH, New York, 2000.
20 J. L. Hardcastle and R. G. Compton, *Electroanalysis*, 2002, **14**, 753.
21 E. Breslow, *Inorganic Biochemistry*, Elsevier, Amsterdam, 1973, **Vol. 1**, p. 227.